OLD DOMINION UNIVERSITY

I-Optimal Split-Plot Design for EVTOL Tilt-Rotor Performance Characterization

Dr. Drew Landman

Professor

Department of Mechanical and Aerospace Engineering

dlandman@odu.edu

Presented at the StatEase 2021 DOE Summit September 28-29, 2021

Todays Talk

- A practioner's eye view of a split-plot experiment design application for wind tunnel testing
- Hard-to-Change factors are common in wind tunnel testing
  - Resistance to formal experiment design is common as well (!)
  - We are making great progress in education of NASA engineers
  - We are also educating Aerospace Engineers thru the AIAA
- In the next 40 minutes I will review a recent study with description of methods and results featuring Design Expert Software
- The heavy lifting for this work was performed by graduate student Michael Stratton at Old Dominion University for his Master's degree
- Financial support from NASA Langley

2

Why Use Tilt-Rotors?

- Vertical Takeoff and Landing (VTOL) with ability to transition to forward flight
- Urban Air Mobility (UAM) is a large emerging aviation market
  - Reduce ground and air traffic congestion, travel times, and emissions
- Combines the maneuverability and flexibility during takeoff and landing of a helicopter with the forward flight efficiency of fixed wing airplanes
- Electric propulsion systems decrease mechanical complexity which allows more freedom in vehicle design
  - Distributed propulsion consisting of may motor/propellors has aerodynamic benefits

3

New Idea ?

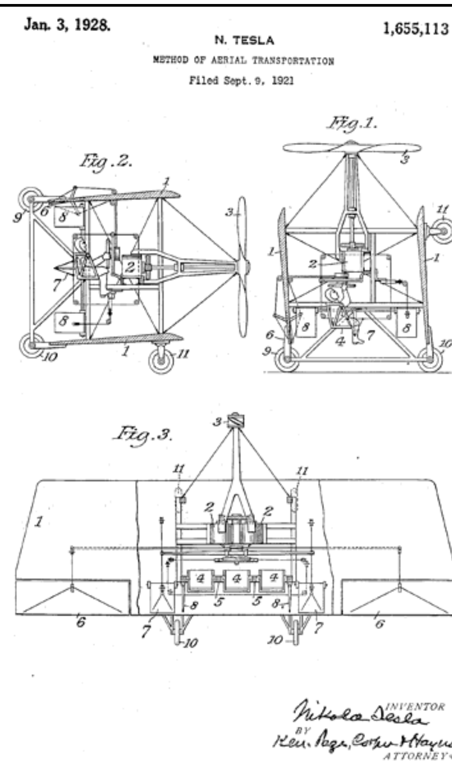

- The Tesla Tilt-Rotor patent of 1929
- Proposed Vertical ascent and descent using propeller
- Tilting wings in flight
- Forward flight sustained using wings
  - Claims lower power required
- Hints at distributed propulsion

4

NASA's New Technology Testbed

- Advanced Air Mobility (AAM) testbed, the Langley Aerodrome 8 (LA-8)
- Distributed electric propulsion
- Tandem tilt-wing eVTOL aircraft

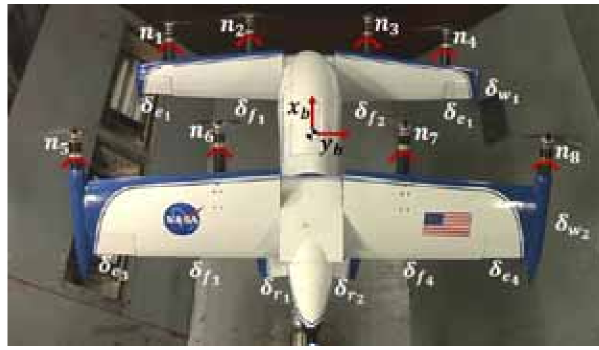

LA-8 prototype in NASA LaRC Wind Tunnel

- Wind tunnel testing methods provide rapid means of characterizing aerodynamic performance
- NASA Langley test program built using statistical engineering featuring DOE, RSM
  - Little historical data, many factors, complex interactions

5

Project Motivation

- eVTOL technology is fairly new and propeller aerodynamics at incidence are not well understood
- Higher blade counts desired as they allow lower rotational speed and hence less noise
- Overall flight modes include hover, transition, forward flight
  - Analytical modeling provides poor predictions
  - Computational methods are complex and arguably not as accurate
  - Wind tunnel experiments needed to gather specific propeller performance data for simulation

6

Project Objectives

- Performance evaluation of the individual LA-8 UAM design candidate propellers in isolation
  - 3, 4, 5, & 6 blade configurations
  - Full performance envelope range of RPM and Angle of Incidence (AOI)
  - Robust statistically defensible math models of propeller performance
    - Anticipated aerodynamic performance models will require higher order terms and interactions
    - Regression models desired for use in flight simulations
    - Bounds on predictions required
- Develop a general testing approach for tilt-rotor characterization

7

Tilt-Rotor Operational Envelope

- Wing and propeller operated at a nominal angle of incidence (α_i) range of 0 - 90°
- Hover (take-off/landing): α_i = 80-90° (82-85° for LA-8)
- Transition: lower α_i
- Forward flight: maximum speed and $\alpha_i \approx 0°$
- Typical eVTOL flight speeds for full scale eVTOL aircraft
  (from Uber Elevate now part of Joby Aviation)

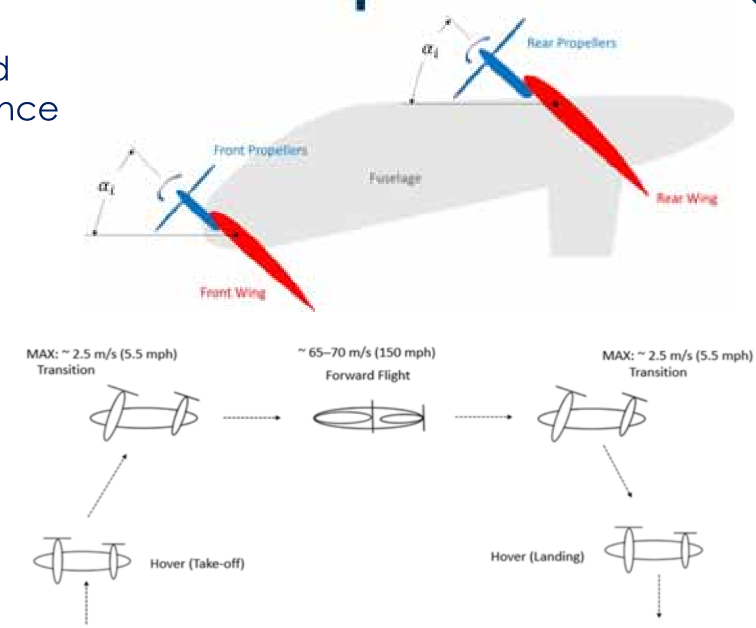

8

Performance Measurement Metrics

- Aerodynamicists choose non-dimensional coefficients for forces and moments
- These are the responses of interest
  - Three Forces
    - Propeller thrust (F_x)
    - Side force (F_y)
    - Normal force (F)
  - Three Moments
    - Propeller torque (M_x)
    - Pitching moment (M_y)
    - Yawing moment (M)

C C C

C C C

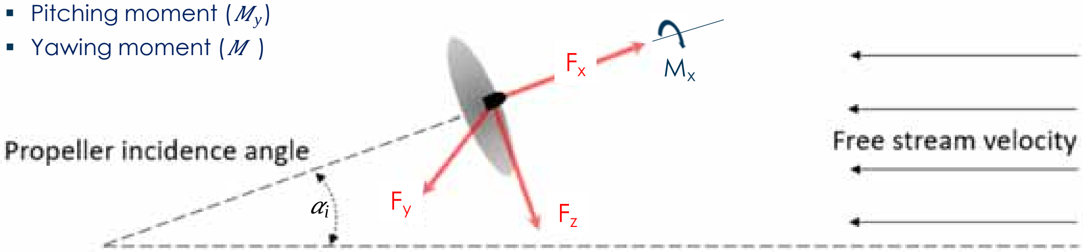

Experimental Details

- The Old Dominion University Low-Speed Wind Tunnel
  - Closed circuit
  - 125-hp motor
  - Low-Speed:
    - 7ft x 8ft test section
    - Max V_∞ 12 m/s
  - High-Speed:
    - 3ft x 4ft
    - Max V_∞ 55 m/s
- Data collected in both sections to build a complete operational envelope

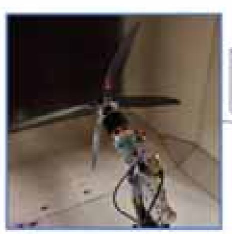

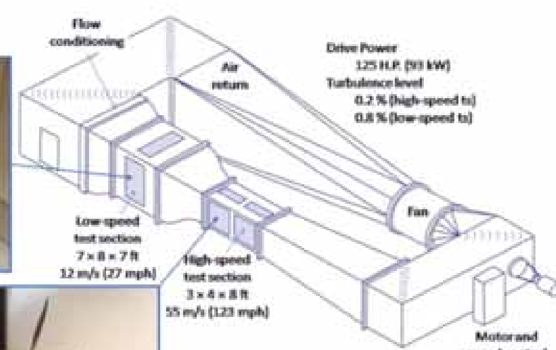

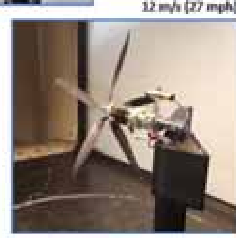

Experimental Details

- Motor support designed to be robust to vibrations
  - Angle of incidence sector with holes staggered and spaced in 10-degree increments from 0 to 180°
- RPM sensor mounted to lever arm, retroreflective laser diode
- Brushless electric motor
  - Same as used on LA-8
- DC power supply
- Force and moment data measured by strain gage load cell

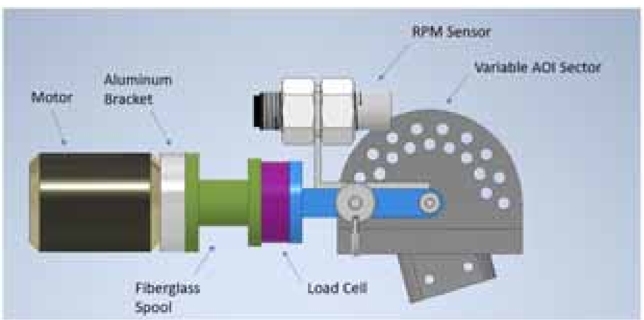

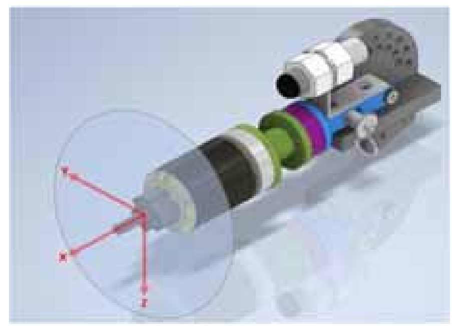

11

Experimental Details

- LA8 model uses Aeronaut CAM Carbon16x8 folding propellers
- 3,4,5, and 6 blade propeller configurations desired
- High blade count for low-noise potential

12

Experimental Details

- Data Acquisition through a PC-based data acquisition board using custom LabVIEW software
- Record & Monitor
  - RPM
  - Test section temperature
  - Test section velocity
  - Motor temperature
  - Motor current
  - Motor voltage
  - Force and moment coefficients

13

Low-Speed Design Space Exploratory Runs

- Test objective
  - To facilitate exploration of design space limits
  - For corroboration with existing data
- Three factors:
  - Tunnel velocity
  - Propeller angle of incidence (AOI) α_i
  - Motor RPM
- Factor levels for tunnel velocity were 0 m/s, 6 m/s, and 12 m/s and AOI from 0° to 100 ° in increments of 20 °
- OFAT: One factor, RPM, was varied while other two were held constant

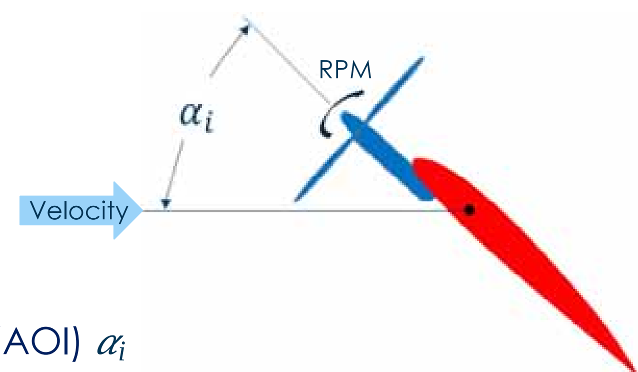

14

Exploratory Runs: Comparison to NASA Data

- 3-Blade thrust and torque coefficient at AOI of 0° shown here
- An important part of designing any experiment
  - Draw on all results from all previous work
  - Establish factor limits for the design space

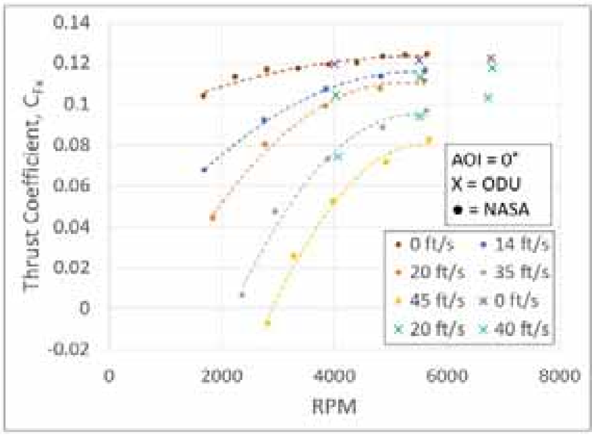

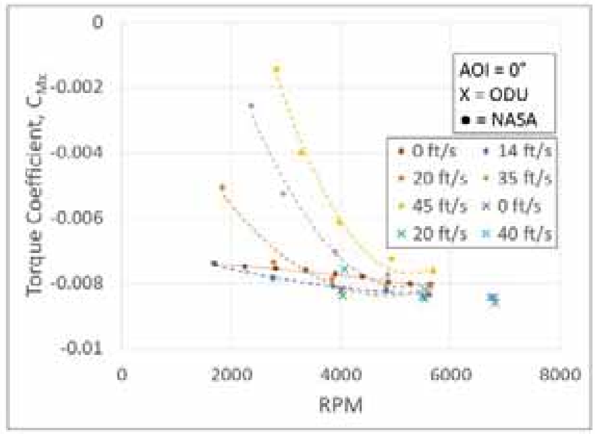

15

Experiment Planning: Low Speed Design

- Primary objective is accurate prediction of force and moments
  - Classical designs would not support anticipated high order models
  - Lends itself to the I-optimal approach – minimize average variance of prediction
- Break factors into easy and hard to change, limits here for 4-blade prop

Name	Change	Low	High	Units
Velocity	Easy	2	12	m/s
AOI	Hard	0	100	deg
RPM	Easy	4000	6500	-

- Choose potential model order based on exploratory runs
  - Fourth order modeling
  - While building the design – we chose to support 5th order
    - Extra lack of fit degrees of freedom and potential to increase order if required

16

Split-Plot Design for Low-Speed Testing

- Lessons learned from initial 4-blade split-plot design
  - Recirculation effects at high incidence angles and zero tunnel velocity; velocity range minimum changed from 0 m/s to 2 m/s
  - Limitations of power supply lowered upper RPM limit from 6800 RPM to 6500 RPM
- Constraints of power supply became more limited as blade number was increased so RPM range had to be adjusted for each blade configuration
  - 5-blade: 4000 RPM – 5800 RPM
  - 6-blade: 3000 RPM – 5500 RPM

17

Split-Plot Design for Low-Speed Testing

- First 3 of 8 whole-plots of 4-blade experiment

			ETC	HTC	ETC						
	Group	Run	Factor 1 A:Velocity, m/s	Factor 2 B: AOI, °	Factor 3 C: RPM	Response 1 CF_x	Response 2 CF_y	Response 3 CF_z	Response 4 CM_x	Response 5 CM_y	Response 6 CM_z
Whole Plot	1	1	8.05	40	4971	0.12628	-0.00102	-0.00510	-0.01002	0.00258	-0.00333
	1	2	9.22	40	4048	0.11454	-0.00053	-0.00653	-0.00984	0.00262	-0.00447
	1	3	2.68	40	3979	0.13338	-0.00127	-0.00194	-0.00986	0.00113	-0.00142
	1	4	12.00	40	6468	0.12423	-0.00126	-0.00606	-0.00993	0.00325	-0.00330
	1	5	3.20	40	5761	0.13649	-0.00103	-0.00195	-0.00984	0.00101	-0.00128
	1	6	6.73	40	6296	0.13279	-0.00105	-0.00375	-0.00997	0.00214	-0.00227
Whole Plot	2	7	9.43	90	4725	0.14087	-0.00001	-0.01280	-0.01024	0.00679	-0.00819
	2	8	3.45	90	6271	0.13969	-0.00146	-0.00385	-0.00992	0.00170	-0.00292
	2	9	12.10	90	6368	0.13726	-0.00014	-0.01353	-0.01016	0.00748	-0.00654
	2	10	2.08	90	5650	0.13906	-0.00093	-0.00300	-0.00977	0.00116	-0.00256
	2	11	6.59	90	6373	0.13903	-0.00139	-0.00725	-0.01008	0.00377	-0.00447
	2	12	12.13	90	6187	0.13696	-0.00009	-0.01393	-0.01019	0.00766	-0.00664
Whole Plot	3	13	5.30	60	4371	0.13429	-0.00109	-0.00633	-0.00994	0.00245	-0.00394
	3	14	11.00	60	5539	0.13258	-0.00112	-0.01067	-0.01002	0.00431	-0.00451
	3	15	12.07	60	4538	0.12934	-0.00017	-0.01320	-0.01019	0.00481	-0.00631
	3	16	7.16	60	6183	0.13541	-0.00177	-0.00614	-0.00990	0.00300	-0.00325
	3	17	2.08	60	5014	0.13757	-0.00059	-0.00193	-0.00983	0.00077	-0.00163
	3	18	2.36	60	6436	0.13932	-0.00096	-0.00204	-0.00987	0.00065	-0.00128

18

I-optimal Split-Plot Design in DX (3-Blade)

- Started by choosing *Optimal(Custom)* design under *Response Surface/Split-Plot*
- Defined factors and levels and indicated Hard or Easy to change

19

I-optimal Split-Plot Design in DX

- Define the model order
  - We could support up to 5th order
  - Only up to 3rd order shown right for brevity

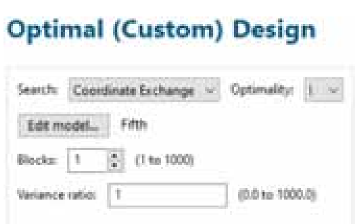

- Choose optimality: I
- Conservative variance ratio of unity chosen
  - WP variance known to be very low due to mechanical design of test rig

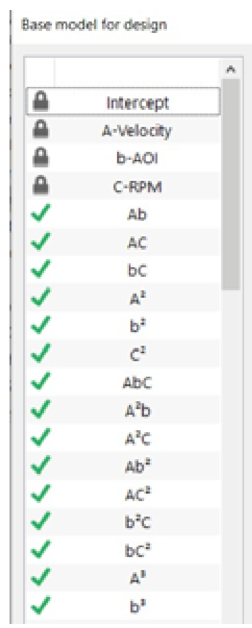

20

I-optimal Split-Plot Design in DX

- Additional whole plots were added in order to increase degrees of freedom for whole-plot term significance testing
  - Here we added 2 to the required 6 groups
- Five additional model points for increased lack of fit degrees of freedom
- Coordinate exchange algorithm for point selection to consider any points in the design space

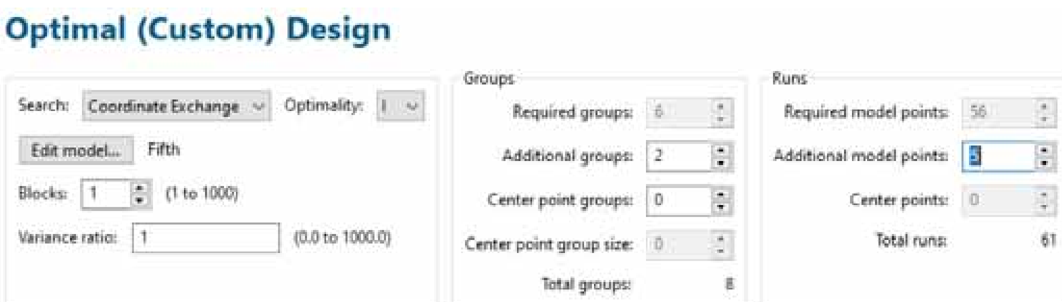

21

I-optimal Split-Plot Design in DX

- 6 responses specified
- After the design is built we adjusted any AOI values that could not be achieved to the next nearest value
  - In hindsight, we should have used factor type *discrete*
- Visualize with *Graph Columns:* design points chosen

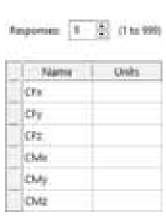

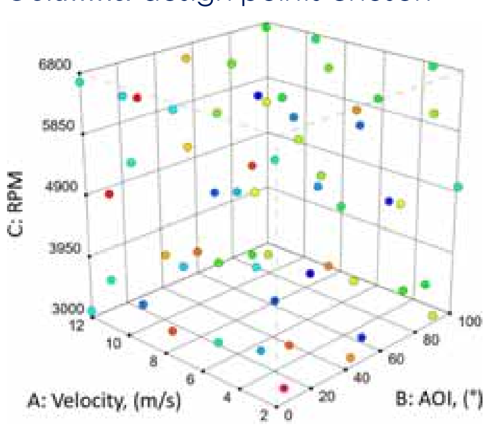

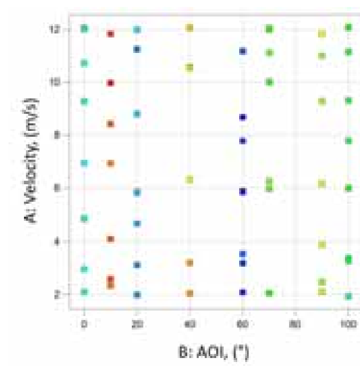

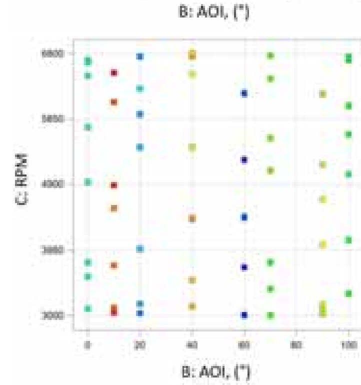

22

I-optimal Split-Plot Design in DX

- Next we used *Evaluation* to review the design metrics
- Use *Evaluation, Results tab,*
  - 4th order model chosen
  - Variance ratio of one – we actually expect this to be lower since the hard to change factor AOI is a very repeatable set point

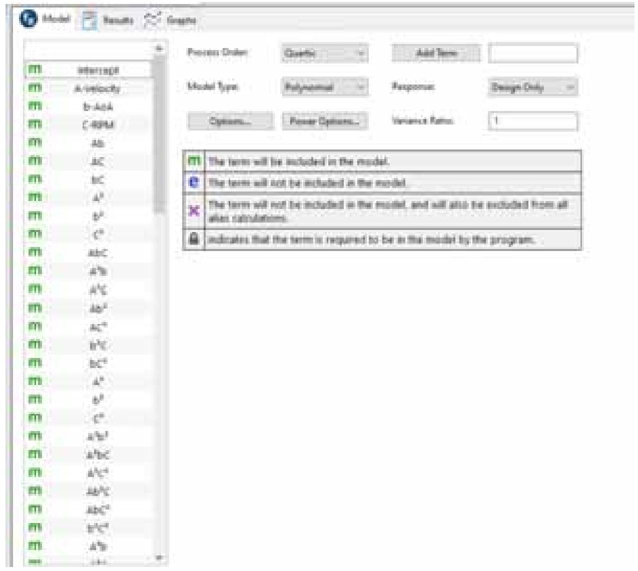

23

I-optimal Split-Plot Design in DX

- We could talk about power but are more interested in the prediction capabilities
  - Prediction variance is of greater interest
- There is some correlation in terms as is always the case when higher order polynomials are used
  - A few terms VIF >20
  - Prediction capabilities are of greater interest and we accept the correlation
- 3 whole-plot error df, 23 subplot error df
- df overhead for support of 5th order, if required

Split-plot Degrees of Freedom

Source	df
Whole-plot	
Model	4
Corr Total	7
Subplot	
Model	30
Corr Total	53

Term	Standard Error*	Error df†	VIF	Restricted‡ VIF	Power
Whole-Plot					
b	1.6684	3.0000	15.448	9.7215	7.198 %
b^2	4.2483	3.0000	23.750	17.424	5.338 %
b^3	1.9899	3.0000	11.119	9.2315	6.545 %
b^4	3.9154	3.0000	20.080	16.977	5.398 %
Subplot					
A	0.71160	23.000	16.257	15.982	27.039 %
C	0.71671	23.000	16.367	15.530	26.724 %
Ab	1.2135	23.000	24.488	24.357	12.400 %
AC	1.1859	23.000	23.031	23.333	12.757 %
bC	1.2312	23.000	24.852	23.070	12.183 %
A^2	1.6918	23.000	24.519	24.991	8.753 %
C^2	1.7666	23.000	26.957	27.403	8.437 %
AbC	0.39670	23.000	1.3548	1.3008	67.528 %
A^2b	0.51297	23.000	3.5404	1.4402	46.338 %
A^2C	0.50178	23.000	3.5242	3.3319	47.992 %
Ab^2	0.53294	23.000	3.6556	3.6694	43.573 %
AC^2	0.51665	23.000	3.7118	3.6497	45.811 %
b^2C	0.53856	23.000	3.6818	3.4546	42.838 %
bC^2	0.50964	23.000	3.3869	1.4514	46.822 %
A^3	0.73321	23.000	11.656	11.872	25.751 %
C^3	0.72500	23.000	11.936	11.135	26.227 %
A^2b^2	0.98691	23.000	5.6707	3.6606	16.312 %
A^2bC	0.70708	23.000	3.5625	3.3737	27.322 %
A^2C^2	0.92570	23.000	5.1896	5.4279	17.901 %
Ab^2C	0.76581	23.000	3.9788	3.7028	24.003 %
AbC^2	0.70567	23.000	3.5830	3.5705	27.412 %
b^2C^2	0.99249	23.000	5.9168	3.8515	16.181 %
A^3b	1.0389	23.000	12.231	12.665	15.180 %
A^3C	0.96611	23.000	11.503	11.307	16.817 %
Ab^3	1.0044	23.000	11.491	11.381	15.910 %
AC^3	1.1204	23.000	12.310	13.972	13.717 %
b^3C	1.0314	23.000	11.690	11.127	15.332 %
bC^3	1.0123	23.000	12.019	11.237	15.736 %
A^4	1.4784	23.000	21.790	22.473	9.940 %
C^4	1.5332	23.000	22.785	24.141	9.586 %

24

I-optimal Split-Plot Design in DX

- Distribution of prediction variance: *Evaluation, graphs tab*
  - Relatively uniform distribution of prediction variance

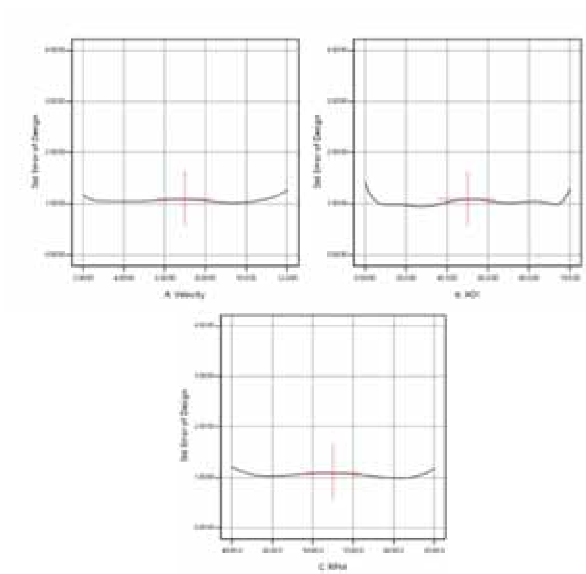

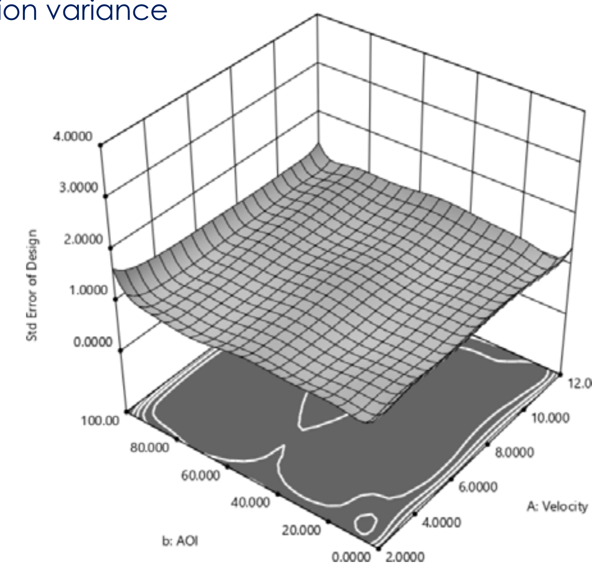

25

I-optimal Split-Plot Design in DX

- When the goal is characterization, the emphasis is on producing a fitted surface as precisely as possible
- Fraction of Design Space analysis used in lieu of power
- In DX
  - **delta** interval half-width
  - **sigma** population standard deviation
  - **alpha** significance level as per usual
- Here we see 95% of the design space has a mean response with a confidence interval half width d ≤ 2.31 for a standard deviation of 1

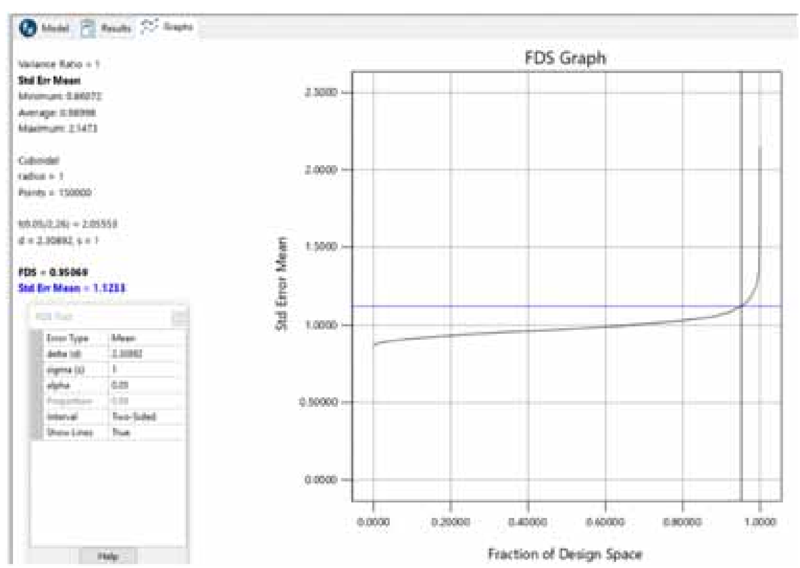

26

Analysis in DX

- ANOVA with Restricted Estimated Maximum Likelihood
  - Starting with the quartic model and using backward elimination
- Models are highly non-linear
- Fit statistics R^2 and R_{adj}^2 are very high with exception of C_{F_y} which is known to be very small in magnitude from theory
- Residual plots confirm normality, indep, const var

	3-Blade		4-Blade		5-Blade		6-Blade	
	R^2	Adjusted R^2	R^2	Adjusted R^2	R^2	Adjusted R^2	R^2	Adjusted R^2
CFx	0.9958	0.9924	0.9977	0.9951	0.9958	0.9928	0.9985	0.9968
CFy	0.9545	0.9189	0.9675	0.9276	0.8588	0.8128	0.9169	0.8753
CFz	0.9852	0.9765	0.9957	0.9931	0.9912	0.9869	0.9908	0.9825
CMx	0.9703	0.9502	0.9642	0.9373	0.9720	0.9620	0.9859	0.9748
CMy	0.9604	0.9389	0.9965	0.9940	0.9939	0.9916	0.9956	0.9922
CMz	0.9982	0.9972	0.9721	0.9573	0.9970	0.9948	0.9960	0.9942

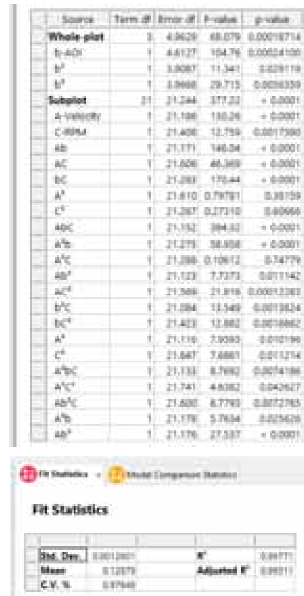

Source	Term df	Error df	F-value	p-value
Whole-plot	3	4.9629	68.079	0.00018714
b-AOI	1	4.6127	104.76	0.00024100
b^2	1	3.0087	11.341	0.028119
b^3	1	3.9666	29.715	0.0058339
Subplot	21	21.244	377.22	< 0.0001
A-Velocity	1	21.166	150.26	< 0.0001
C-RPM	1	21.408	12.759	0.0017380
Ab	1	21.171	146.04	< 0.0001
AC	1	21.606	46.369	< 0.0001
bC	1	21.283	170.44	< 0.0001
A^2	1	21.610	0.79781	0.38159
C^2	1	21.267	0.27310	0.60666
AbC	1	21.152	384.02	< 0.0001
A^2b	1	21.275	58.958	< 0.0001
A^2C	1	21.266	0.10612	0.74779
Ab^2	1	21.123	7.7373	0.011142
AC^2	1	21.566	21.816	0.00012283
b^2C	1	21.084	13.549	0.0013624
bC^2	1	21.423	12.882	0.0016862
A^3	1	21.116	7.9593	0.010196
C^3	1	21.647	7.6861	0.011214
A^2bC	1	21.133	8.7692	0.0074186
A^2C^2	1	21.741	4.6382	0.042627
Ab^2C	1	21.600	8.7793	0.0072765
A^3b	1	21.179	5.7634	0.025626
Ab^3	1	21.176	27.537	< 0.0001

Fit Statistics · Model Comparison Statistics

Fit Statistics

Std. Dev.	0.0012601	R^2	0.99771
Mean	0.12379	Adjusted R^2	0.99511
C.V. %	0.97648		

Sample Results: Thrust Coefficient C_{Fx}, AOI = 0

- Effect of RPM on thrust coefficient at 0° AOI over velocity range tested
  - This is the forward flight mode
  - Thrust coefficient decreases with increase in airspeed as per theory
  - Decreases more quickly at lower RPM – a classic interaction
  - An increase in blade number increases thrust coefficient – more blades mean more lift force created
  - Confidence intervals on mean response at 95% shown
- Experiments provide detail and quantify precision not possible with theoretical approach

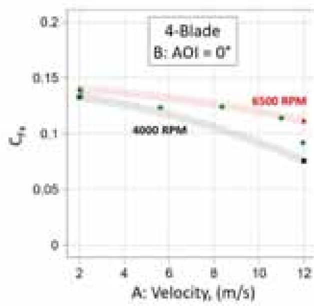

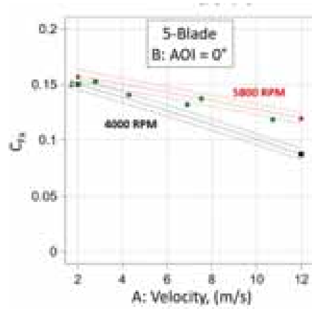

Sample Results: Thrust Coefficient, C_{Fx}, AOI = 60

- Decrease in thrust coefficient with increased airspeed not as severe as incidence angle is increased
- Interaction effect with RPM is now essentially absent
- While these trends are predicted by theory the true values are hard to predict accurately and the critical AOI (60) may be different
- Experiments such as this are required for accurate flight simulation

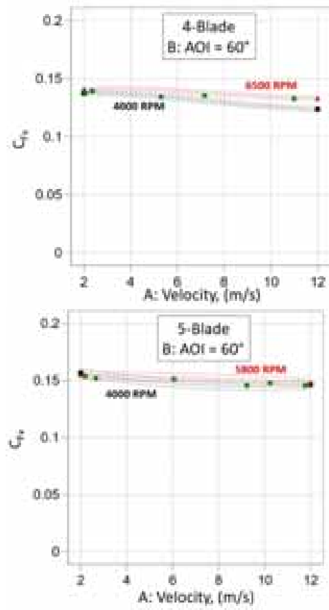

Sample Results: Pitching Moment Coefficient Response

- Pitching moment grows significantly
  - As AOI nears 90°
  - Effect amplified by higher velocity
- Very important result for aircraft stability and control

Pitching moment coefficient at 5000 RPM

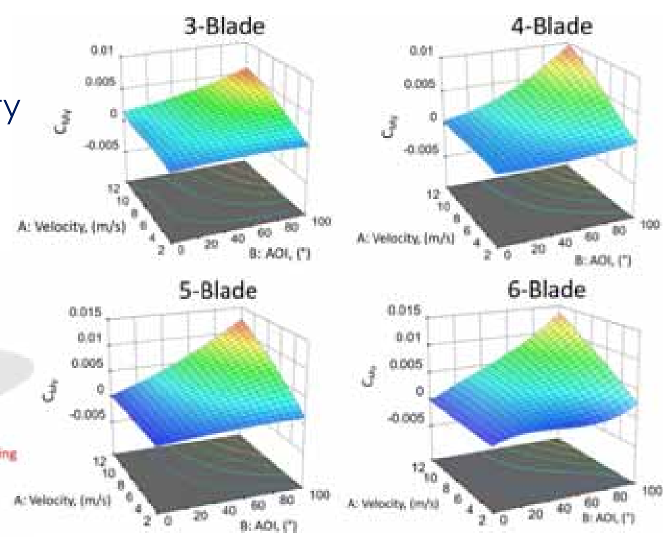

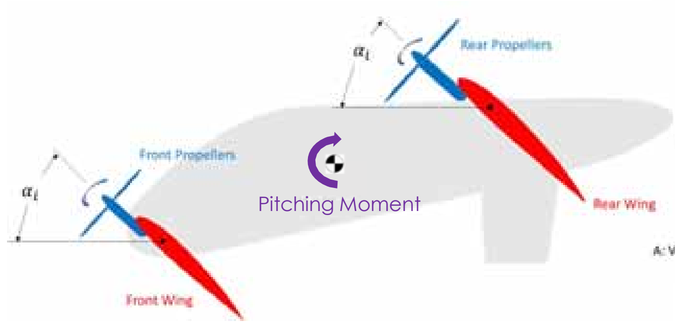

Design Development for High-Speed Testing

- AOI now limited to 0-20 degrees
- Windmill condition led to constraints on design space in RPM and velocity
  - When the prop thrust = 0
- Red line shows approximate limits in RPM – Velocity Space
  - Easy in DX:

high-level of factor A (velocity) low-level of factor C (RPM)

$$1 \leq \frac{HL_A - A}{HL_A - CP_A} + \frac{C - LL_C}{CP_C - LL_C}$$

constraint point of factor A constraint point of factor C

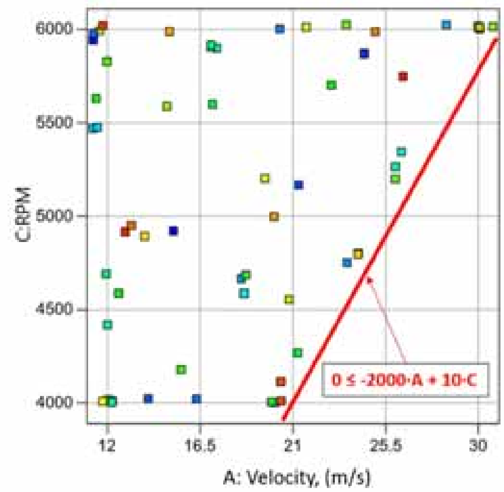

DX I-optimal Split-Plot Design for High-Speed Testing

- Same I-optimal split-plot design approach but now with four factors
- Results from exploratory tests suggested a 3rd order model would be sufficient
- Limited degrees of freedom in AOI
  - Reduced number of levels (3) – second order in AOI
  - Lower incidence angles representative of transition flight mode; recall eVTOL flight envelope figure
- Blade number added as categorical factor
  - Increased run efficiency
  - HTC factor
  - Robust comparisons of blade count
- Factors, levels types as entered in DX Split Plot Optimal Response Surface

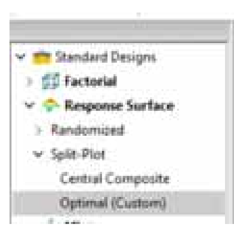

	Name	Units	Change	Type	Levels	L[1]	L[2]	L[3]	L[4]
A [Numeric]	Velocity		Easy	Continuous	N/A	11	30		
b [Numeric]	AOI		Hard	Continuous	N/A	0	20		
C [Numeric]	RPM		Easy	Continuous	N/A	4000	6000		
d [Categoric]	Blades		Hard	Nominal	4	3	4	5	6

DX I-optimal Split-Plot Design for High-Speed Testing

- First 4 of 17 whole plots shown
- Note there are now 2 Hard-to-Change (HTC) and 2 Easy-to-Change (ETC) factors

			ETC	HTC	ETC	HTC						
	Group	Run	Factor 1 A:Velocity, m/s	Factor 2 B:AOI, °	Factor 3 C:RPM	Factor 4 D:Blades	Response 1 CF_x	Response 2 CF_y	Response 3 CF_z	Response 4 CM_x	Response 5 CM_y	Response 6 CM_z
Whole Plot	1	1	15.21	10	4921	6	0.10117	0.00043	-0.00493	-0.01151	0.00011	-0.00239
	1	2	11.30	10	5943	6	0.14442	0.00045	-0.00376	-0.01369	0.00027	-0.00197
	1	3	24.46	10	5874	6	0.05078	0.00052	-0.00508	-0.00747	0.00050	-0.00259
	1	4	24.45	10	5868	6	0.05054	0.00056	-0.00507	-0.00746	0.00050	-0.00261
Whole Plot	2	5	21.28	10	5167	4	0.03962	0.00035	-0.00439	-0.00542	0.00034	-0.00197
	2	6	13.98	10	4023	4	0.06313	0.00072	-0.00365	-0.00733	0.00014	-0.00196
	2	7	11.32	10	5978	4	0.11100	-0.00010	-0.00176	-0.00963	0.00056	-0.00122
Whole Plot	3	8	16.32	20	4022	3	0.04929	-0.00003	-0.00692	-0.00593	0.00042	-0.00308
	3	9	20.35	20	6004	3	0.06572	0.00021	-0.00455	-0.00679	0.00131	-0.00288
	3	10	23.63	20	4752	3	0.01915	0.00047	-0.00923	-0.00333	0.00032	-0.00370
Whole Plot	4	11	18.49	20	4665	6	0.07466	0.00117	-0.00985	-0.00941	0.00110	-0.00490
	4	12	28.44	20	6024	6	0.03389	0.00161	-0.01182	-0.00587	0.00111	-0.00514
	4	13	11.30	20	5470	6	0.14316	-0.00021	-0.00526	-0.01344	0.00161	-0.00285

DX I-optimal Split-Plot Design for High-Speed Testing

- Reviewing the design metrics in *Evaluation*
  - Five whole-plot error degrees of freedom
  - Eight subplot error degrees of freedom
    - Fewer degrees of freedom then previous design but more than adequate
  - Same issues with correlation
- Same objectives
  - Emphasis is on prediction

Source	df
Whole-plot	
Model	11
Corr Total	16
Subplot	
Model	37
Corr Total	45

Term	Standard Error*	Error df+	VIF
Whole-Plot			
b	0.5211	5	6.31796
d[1]	1.11	5	
d[2]	0.9315	5	
d[3]	0.8908	5	
bd[1]	0.6028	5	
bd[2]	0.7255	5	
bd[3]	0.7631	5	
b^2	0.7915	5	4.21827
b^2d[1]	1.21	5	
b^2d[2]	1.07	5	
b^2d[3]	1.13	5	
Subplot			
A	1.04	8	21.9615
C	1.44	8	61.9669
Ab	0.6922	8	7.79178
AC	2.06	8	45.2874
Ad[1]	0.7705	8	
Ad[2]	0.7557	8	
Ad[3]	0.9388	8	
bC	0.5024	8	5.49176
Cd[1]	0.6000	8	

DX I-optimal Split-Plot Design for High-Speed Testing

- In DX: *Evaluation, Graphs*
- Reviewing the 3D surface plots for prediction variance
  - I-Optimal design helps ensure a reasonably uniform distribution of prediction variance in a constrained space

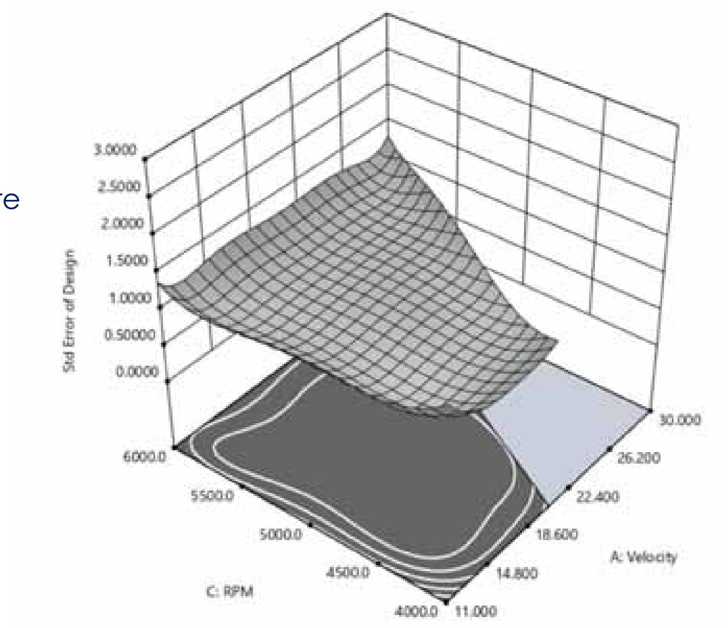

35

High-Speed Split Plot Analysis in DX

- Experiments analyzed in DX using Analysis of Variance with REML at 95% confidence
- Estimates of whole-plot and sub-plot variance components
  - Whole-plot error was found to be small due to the repeatability of WP factors (blades and AOI)
- Results for C_{F_X} response (thrust)
  - Group (WP) < half magnitude of residual (SP)

Configure | Model | ANOVA (REML) | Diagnostics | Model Graphs

Fixed Effects [Type III] | Variance Components

Variance Components

Source	Variance	Standard Error	95% CI Low	95% CI High
Group	6.3141E-07	6.1876E-07	-5.8134E-07	1.8442E-06
Residual	1.5819E-06	4.7386E-07	9.4895E-07	3.1521E-06
Total	2.2133E-06			

Response 1: CFx

REML (REstricted Maximum Likelihood) analysis
Kenward-Roger p-values

Source	Term df	Error df	F-value	p-value	
Whole-plot	8	10.22	126.83	< 0.0001	significant
b-AOI	1	7.99	422.57	< 0.0001	
d-Blades	3	21.26	125.49	< 0.0001	
bd	3	7.26	11.03	0.0043	
b²	1	9.91	34.09	0.0002	
Subplot	23	23.06	2623.37	< 0.0001	significant
A-Velocity	1	26.25	6838.02	< 0.0001	
C-RPM	1	24.10	943.18	< 0.0001	
Ab	1	24.02	72.01	< 0.0001	
AC	1	28.12	287.00	< 0.0001	
Ad	3	23.64	302.21	< 0.0001	
bC	1	24.72	31.44	< 0.0001	
Cd	3	25.07	72.78	< 0.0001	
A²	1	26.22	70.31	< 0.0001	
C²	1	26.94	203.16	< 0.0001	
ACd	3	23.28	16.04	< 0.0001	
A²C	1	28.50	7.44	0.0108	
AC²	1	29.29	38.12	< 0.0001	
b²C	1	23.21	6.08	0.0215	
C²d	3	23.17	3.91	0.0215	
C³	1	25.03	4.29	0.0488	

36

Results: High-Speed Force and Moment Coefficient Responses

- Easy comparison between blade-counts
- Similar trends compared to low-speed experiments for range of AOI tested
- Thrust coefficient decreases with increase in airspeed
- Minor increases in thrust coefficient at AOI = 20 ° vs 0 ° - note 5 and 6-blade
- 3-blade shows unexplained minor increase compared to 4-blade – may be due to a difference in the hinged blade fasteners
- Torque coefficient decreases as a result of a decrease in thrust coefficient for all blade configurations as expected

Thrust coefficient at 6000 RPM

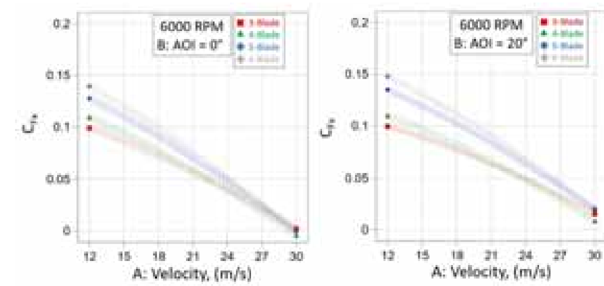

Torque coefficient at 6000 RPM

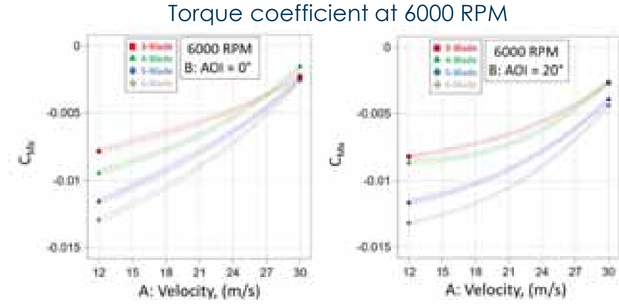

37

Results: High-Speed Pitching Moment Coefficient Responses

- Overall similar trends to low-speed results over the 0<AOI<20 range with exception of 3-blade
- Noticeable difference in trend for 3-blade led to investigation
  - Increased spread in residuals found for 3-blade vs others
  - May be due to a difference in the hinged blade fasteners

Pitching moment coefficient at 6000 RPM

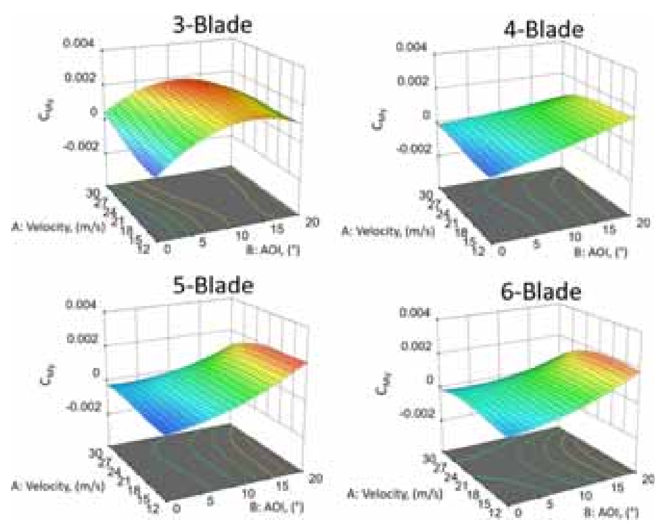

38

Conclusions

- The split plot design approach provided practical experiment efficiency
  - While still incorporating necessary randomization and minimizing variance
  - HTC factor changes were very repeatable (AOI and blade count) hence WP variance was low
- Only a very small portion of the results were shown – much insight was gained
- A complete simulation database was created from the five tests described here
  - One each 3,4,5,6 low-speed test and one aggregate high-speed test
- The database will be used with a full flight vehicle simulation in the future
- This project showcased important tools for aerospace engineers who have traditionally been reluctant to use DOE/RSM
- Design Expert software was used throughout
  - Design creation
  - Design evaluation
  - Design analysis and model building
  - Model presentation and interpretation

References

Stratton, M., Landman, D., "Wind Tunnel Test and Empirical Modeling of Tilt-Rotor Performance for EVTOL Applications," AIAA SciTech 2021 Forum, https://doi.org 10.2514/6.2021-0834

Simmons, B. M., and Murphy, P. C., "Wind Tunnel-Based Aerodynamic Model Identification for a Tilt-Wing, Distributed Electric Propulsion Aircraft," AIAA SciTech 2021 Forum, https://doi.org/10.2514/6.2021-1298

Busan, R. C., Murphy, P. C., Hatke, D. B., and Simmons, B. M., "Wind Tunnel Testing Techniques for a Tandem Tilt-Wing, Distributed Electric Propulsion VTOL Aircraft," AIAA SciTech 2021 Forum, https://doi.org/10.2514/6.2021-1189

Murphy, P. C., Simmons, B. M., Hatke, D. B., and Busan, R. C., "Rapid Aero Modeling for Urban Air Mobility Aircraft in Wind-Tunnel Tests," AIAA SciTech 2021 Forum, https://doi.org/10.2514/6.2021-1644